JMEPEG (2010) 19:1005–1014
DOI: 10.1007/s11665-009-9583-7

1059-9495/$19.00

Effect of Cyclic Aging on Mechanical Properties and Microstructure of Maraging Steel 250

Fawad Tariq, Nausheen Naz, and Rasheed Ahmed Baloch

(Submitted April 1, 2009; in revised form September 2, 2009)

The effects of thermal cyclic aging on mechanical properties and microstructure of maraging steel 250 were studied using hardness tester, tensile testing machine, impact tester, optical, scanning electron, and stereo microscopy. Samples were solution annealed at 1093 K for 1 h followed by air cooling to form bcc martensite. Cyclic aging treatments were carried out at 753 and 773 K for varying time periods. Increase in hardness and strength with corresponding decrease in ductility and impact strength was observed with increasing aging cycles. Reverted austenite was detected by x-ray diffraction technique formed as a result of cyclic aging. The presence of reverted γ was also confirmed by EDX-SEM analysis and attributed to the formation of Mo- and Ni-rich regions which transformed to γ on cooling. Heterogeneity in composition and amount of reverted γ was found to increase with increase in aging cycles and aging time. Fractography reveals the change in fracture mode from ductile dimple-like to brittle cleavage with increase in hardness and strength due to cyclic aging.

Keywords aging, heat treatment, maraging steel, martensite, precipitation, reverted austenite

1. Introduction

The 18% Ni maraging steel is based on the binary Fe-Ni system with additions of various alloying elements such as Co, Mo, Ti, and Al for precipitation hardening. These steels are classified as materials of ultrahigh strength combined with good toughness (Ref 1-4), which maintain their properties at temperatures up to at least 623 K. As such, they constitute an alternative to hardened carbon steels in critical applications where high strength and good toughness and ductility are required. They harden by a simple and relatively low-temperature maraging treatment at 753 K for 3-8 h followed by air cooling (Ref 5, 6). Upon cooling an 18 Ni alloy from the austenitic range, the austenite (γ) transforms to a lath martensite by a diffusionless shear reaction that has a 100% bcc crystal structure with high dislocation density but no twinning (Ref 4, 7). During aging heat treatment, high strength is achieved by precipitation of a high amount of intermetallic compounds (like Fe_2Mo, Ni_2Mo, Ni_3Mo, Ni_3Ti, Fe_7Mo, etc.; depending upon the alloying elements and aging treatment) dispersed in a carbonless martensitic matrix supersaturated with alloying elements (Ref 1, 8-10). More than one precipitate could exist in maraging steel depending upon aging kinetics (Ref 8). The aging process developed in stages and is accompanied by corresponding structural changes.

Fawad Tariq, Nausheen Naz, and **Rasheed Ahmed Baloch**, Materials Research and Testing Laboratory, Pakistan Space and Upper Atmosphere Research Commission (SUPARCO), Karachi, Pakistan. Contact e-mail: t_fawad@hotmail.com.

Hardness in the range of about 540-550 HV, tensile strength in between 1750 and 1800 MPa, and elongation in between 6-6.5% was achieved earlier in maraging steel grade 250 sheets after aging at 753 K for 3 h. However, in a sheet of similar composition but from different heat (production route for both sheets were same) under study, required hardness and strength were not achieved after standard aging treatment. Even raising the aging temperature up to 773 K and time to 6 h was not found effective in obtaining desired set of mechanical properties. Peak hardness of about 485 HV and strength about 1575 MPa was achieved after 5 h of aging at 773 K. Traditional method for improving mechanical properties of maraging steel is refining grain size by thermal cycling in γ field or α + γ field. Though considerable work has been carried out in the past in generating data on the mechanical and metallographic properties of maraging steel 250, no significant information is available in the open literature on the mechanical properties and microstructural characteristics of 250 grade of maraging steel as a result of interrupted and cyclic aging below austenite start (A_s) temperature. Most of the studies on maraging steels are confined to either the effect of single step aging treatments following solution heat treatment (Ref 11-14) or thermal cycling in $\alpha \rightarrow \gamma$ range (Ref 14-19) or thermal cycling in dual phase α + γ range like in welding (Ref 20-23) on mechanical and metallurgical properties. Furthermore, most of the aging heat treatments are carried out in electric-resistance furnaces and power failure or any malfunctioning in the furnace will cause interruption in thermal aging treatment the result of which on mechanical and metallurgical properties is not known yet. It is therefore of considerable interest to study the effect of cyclic or interrupted aging treatments (below the A_s temperature) on mechanical properties and microstructures of maraging steel 250.

This paper discusses the results of experiments carried out on maraging steel grade 250 sheet to evaluate the effects of cyclic aging treatments at 753 and 773 K with varying aging times on mechanical properties and evolution of microstructure.

2. Experimental Work

The study was undertaken on a sheet of 18% Ni maraging steel grade 250 that was produced in electric arc furnace followed by vacuum degassing and electro-slag remelting to reduce the impurity level and yield ultra-clean steel. Ingot was then hot rolled to approximately 5.5 mm thickness. The chemical composition of the maraging steel grade 250 used in this investigation is given in Table 1.

Square samples of around 2 in. with 5 mm thickness were cut from the sheet for heat treatments and were solution annealed at 1093 K for 1 h followed by air cooling to room temperature. The ASTM grain size number of the sheet in solution annealed condition was measured to be approx. 8 (grain diameter about 20-23 μm). As the objective of the present investigation was to find out the effect of cyclic aging on mechanical properties and microstructure, various thermal cyclic aging treatments were formulated. Since it is well known that reversion of austenite and coalescence of precipitates occurs above 773 K in maraging steels (Ref 5, 6), the study was confined to standard aging temperatures of 753 and 773 K. However, aging time for each cycle was kept different. All samples were air cooled to room temperature after each cycle. Complete outline of the experimental procedure for cyclic aging is shown in Table 2. All treatments were carried out in electric resistance batch-type furnace at a heating rate of 25 K/min. Temperature variation during heat treatments was kept within ±278 K.

Vickers hardness measurements, made with a 100 kg load for 30 s on a suitably prepared surface, were used to monitor hardness changes during all cyclic aging treatments. The hardness data reported in this paper represent the average of at least five measurements per sample keeping in view the possibility of segregation or other defects. In order to evaluate the effect of cyclic aging on strength and ductility, tensile testing was carried out after each aging cycle. Tension tests were conducted on sheet specimens of standard size of 50 mm gauge length, 12.7 mm width, and 5 mm thickness as per ASTM E 8-99 cut from the longitudinal direction. All the tension tests were performed on a 250 KN universal tensile testing machine at a loading rate of 0.50 KN/s at room temperature. Percentage elongation in each specimen was measured by using strain gauge-based extensometer. Average of at least two tensile tests for each testing condition is reported here. Impact tests were also carried out on Charpy V-notch standard sub-size specimens of 5 × 10 × 55 mm as per ASTM E 23-98. Fractographic observations were made on fractured Charpy V-notch specimens using a stereomicroscope at a magnification of 15× and JEOL JSM-6380A analytical scanning electron microscope (SEM) to determine the type and mode of fracture.

In addition to mechanical testing, metallographic examination was carried out on all treated samples using optical microscope and JEOL scanning electron microscope (SEM) equipped with energy dispersive x-ray (EDX) spectrometer. Metallographic samples were prepared by adopting standard mounting, mechanical grinding, and polishing techniques. Observations were made after etching with a 5% nital solution. Quantitative measurements of the amounts and types of phases present, after the above heat treatments, were carried out using a Bruker AXS D-8 Advance x-ray diffractometer. All the x-ray measurements were carried out at room temperature in step scan mode with a step size of 0.02, time per step of 3 s, and angular interval 45-90°. CuKα (1.54056 Å) radiation filtered with Ni was used with 40 kV and 40 mA without monochromator. Austenite and martensite quantification was carried out by direct comparison method (Ref 24).

Table 1 Chemical composition (in wt.%) of maraging steel grade 250 sheet

C	Si	Mn	Ni	Co	Mo	Ti	Al	S	P	Fe
0.01	0.06	0.03	17.97	7.97	5.03	0.50	0.11	0.008	0.005	Bal.

3. Results

The response of cyclic (interrupted) aging treatments on hardness, tensile strength, ductility (in terms of elongation), and Charpy V-notch impact energy with varying time of aging were plotted on graph for each sample, as shown in Fig. 1.

Figure 1 exhibits the mechanical properties of maraging steel 250 plotted against sample number, which were cyclic aged for different time periods at 753 and 773 K. An increase in hardness and strength in response to the number of aging cycles are observed in Fig. 1(a) and (b). Hardness gain in the range of 15-20% and strength gain in the range of 19-25% was attained as a result of four aging cycles. However, increase in hardness with aging cycles was not constant and varying hardness values were observed as time of aging for 1st cycle was changed from 0.25 h (sample S1) to 1.75 h (sample S7). It can be seen in Fig. 1(a) that hardness curve gradually rises with aging time for samples aged for 0.25 h (S1) up to 0.75 h (S3) and then drops from aging time of 0.75 h (S3) down to 1.25 h (S5) and then again rise with aging time up to 1.75 h (S7).

Table 2 Cyclic age hardening treatments done on maraging steel grade 250 sheet samples

Sample ID	No. of samples	Cyclic age hardening treatments			
		1st aging cycle	2nd aging cycle	3rd aging cycle	4th aging cycle
S1	2	753 K for 0.25 h	753 K for 2.75 h	773 K for 1.5 h	773 K for 1.5 h
S2	2	753 K for 0.50 h	753 K for 2.50 h	773 K for 1.5 h	773 K for 1.5 h
S3	2	753 K for 0.75 h	753 K for 2.25 h	773 K for 1.5 h	773 K for 1.5 h
S4	2	753 K for 1.00 h	753 K for 2.00 h	773 K for 1.5 h	773 K for 1.5 h
S5	2	753 K for 1.25 h	753 K for 1.75 h	773 K for 1.5 h	773 K for 1.5 h
S6	2	753 K for 1.50 h	753 K for 1.50 h	773 K for 1.5 h	773 K for 1.5 h
S7	2	753 K for 1.75 h	753 K for 1.25 h	773 K for 1.5 h	773 K for 1.5 h

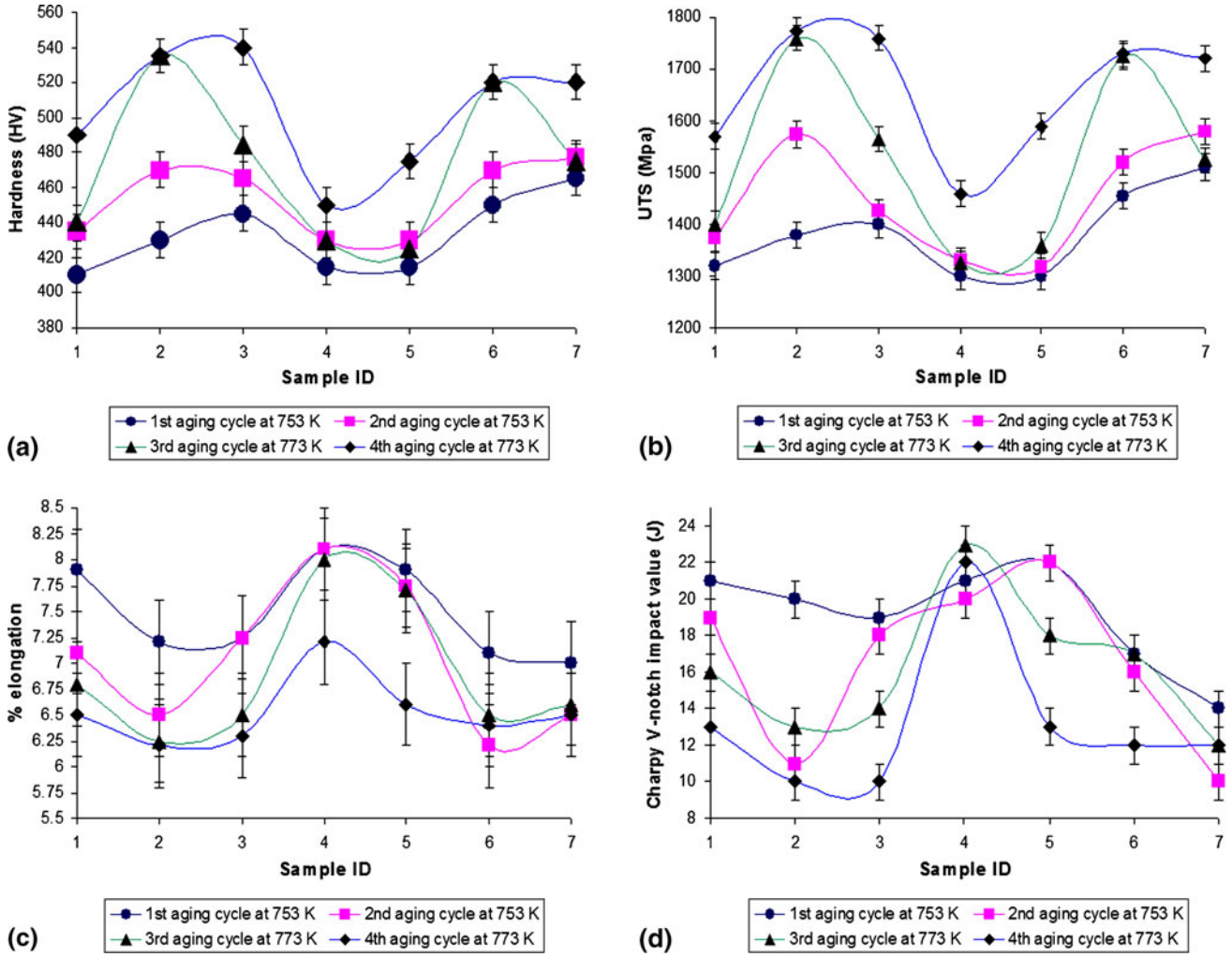

Fig. 1 Graphs showing variation in (a) hardness, (b) ultimate tensile strength, (c) %elongation, and (d) impact absorbed energy in response to cyclic aging and varying aging time

Lowest hardness values were observed for samples aged for the 1st cycle in time range >0.75 h and <1.5 h in comparison to other time periods. Peak hardness of 540 HV was obtained in S3 samples (aged for 0.75 h in 1st cycle) after 4th aging cycle. Similar trend in tensile strength was observed in Fig. 1(b) in response to cyclic aging treatments, i.e. ultimate tensile strength increased with increasing aging cycles for all samples. However, aging time again affects the strength in the same way as hardness, i.e. wave-like curve was obtained due to rise and fall in strength level, depending upon time of 1st aging cycle. Maximum strength of 1770 MPa was achieved in S3 samples after 4th aging cycle just like hardness; since a direct relationship exists between hardness and strength. As ductility (elongation) and impact resistance (toughness) is inversely proportional to hardness and strength; therefore, the curve of %elongation and impact absorbed energy, as shown in Fig. 1(c) and (d), are different from those of hardness and strength, i.e. %elongation and impact energies initially decrease down to 6.2% and 10 J (S3) and then rise to the peak value of 7.2% and 22 J (S4), and then again drops down to 6.5% and 12 J (S7) after 4th aging cycle. Moreover, %elongation and impact absorbed energies were found to decrease with each successive cycle for all temperatures and time periods. Decrease in ductility and toughness (as indicated by %elongation and impact resistance) with corresponding increase in hardness and strength is associated with the precipitation of hardening compounds due to cyclic aging. However, increase in ductility and toughness at higher aging temperatures and longer aging times are attributed to the formation of reverted austenite. As reverted γ is soft and ductile phase in comparison to martensite matrix, the combination of both phases acts as a composite structure. Hence during plastic deformation, soft and ductile reverted γ absorbs more energy prior to fracture than martensite (Ref 1, 5, 6, 25). Therefore, increasing either the aging temperature or time or both will increase the percentage of reverted γ in the structure, which in turn raises the toughness of the steel. However, there is a limit of increasing toughness by increasing % γ because the strength of the material is significantly reduced. It is therefore desirable to limit the % γ to below 15% for achieving optimum mechanical properties (Ref 25-27).

Results of fractography, carried out on fractured Charpy V-notch impact specimens after different cycles of aging for varying aging times by stereomicroscope, are shown in Fig. 2. Depending upon the hardness of the specimen, type of fracture varies from fully ductile (for low hardness values) to fully

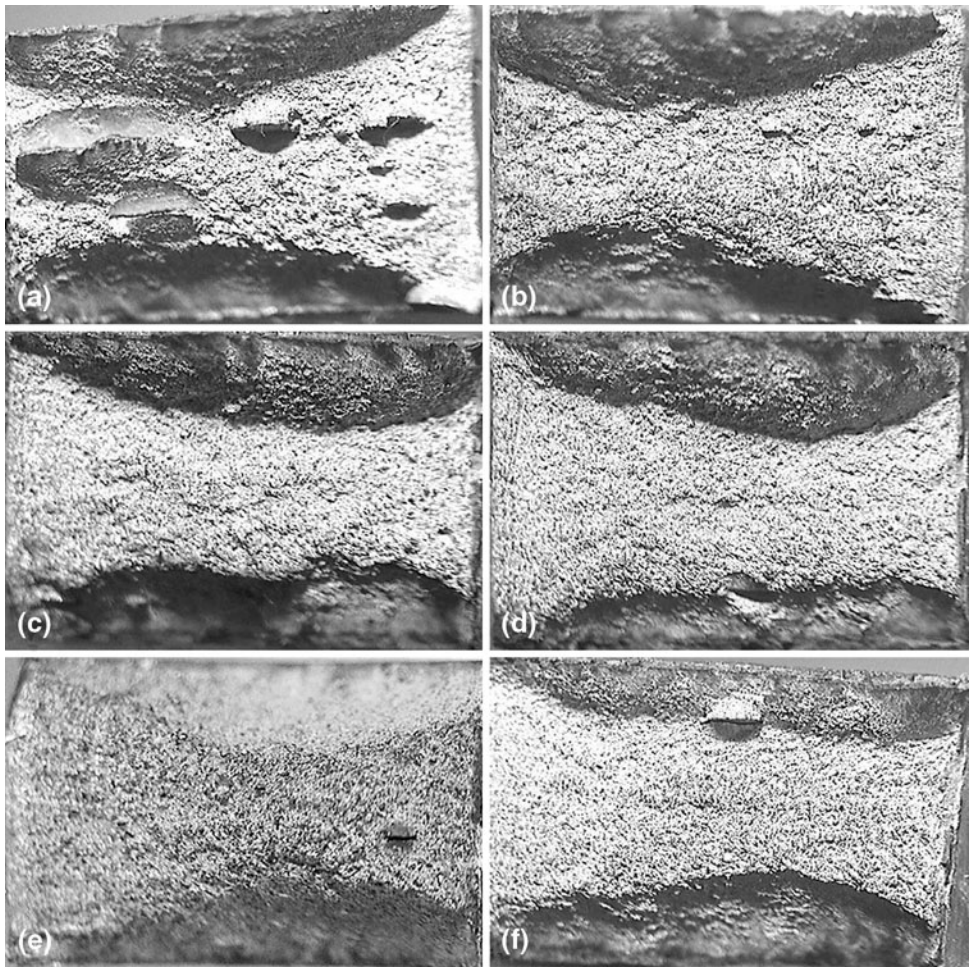

Fig. 2 Fractographs of Charpy V-notch impact specimens showing (a, b) ductile fracture (dull with voids and dimples), (c, d) partially ductile with partially brittle fracture (shinny facet centre—brittle) and (e, f) brittle (cleavage) fracture

brittle (for high hardness values) with partially ductile-brittle fracture for intermediate hardness values.

Figure 2(a) and (b) shows ductile fracture (dull appearance) with voids and dimples for specimens having lower hardness values, while Fig. 2(e) and (f) shows the typical brittle cleavage fracture with bright shiny facets for specimens having higher hardness. Figure 2(c) and (d) shows partially ductile (dull) with partially brittle fracture (shinny centre). Fractographic observations were also made at higher magnification on scanning electron microscope to reveal the mode of fracture as shown in Fig. 3.

It is observed from Fig. 3(a)-(c) for specimens fractured after 2nd aging cycle with different aging times that the mode of fracture is transgranular with small voids and large dimples (some stretched-zones) which were expected to nucleate at inclusions or possibly on reverted γ. Voids or micro-cracks could also be nucleated at precipitate/matrix interface or at areas adjacent to the brittle precipitate. However, detailed examination of fractured surface at higher magnifications did not show any void nucleating at reverted γ or inclusion. It was further observed that different aging treatments did not change the distribution pattern of voids and dimples for ductile fractures. Figure 3(d) shows brittle transgranular fracture with only microvoids; coarser dimples were not present which indicates the brittle nature (lower toughness) of S7 specimen which was cyclic aged for the 2nd time and having impact energy of about 10 J. It was further observed that the fracture appearance changes from ductile-dimple like surface to brittle shinny surface with an increase in the number of aging cycles, i.e. impact energy and thus toughness decreases with increase in aging cycles.

Figure 4 shows the optical micrographs of different samples treated for different number of aging cycles. Figure 4 reveals the typical bcc lath martensitic structure of maraging steel 250 with varying amounts and sizes of reverted austenite (γ), the amount of which depends on the number of aging cycles and time of 1st aging cycle. The amount of γ was found to increase with the number of aging cycles in all samples irrespective of the aging time. This was also confirmed through the results of x-ray diffraction. It was found that the aging time and precipitation process influenced the amount of γ, i.e. the higher the aging time for 1st cycle, the lower will be the γ content. White ribbons of reverted γ were found to nucleate within the grains at martensite lath boundaries due to micro-segregation of alloying elements in these regions and in some cases at prior austenite grain boundaries. Compositional heterogeneity in structure increased with the number of aging cycles, resulting in the formation of alloy-rich (some areas within the grain become enriched with certain elements) and alloy-lean (i.e. areas within the grain depleted of certain elements) regions which on

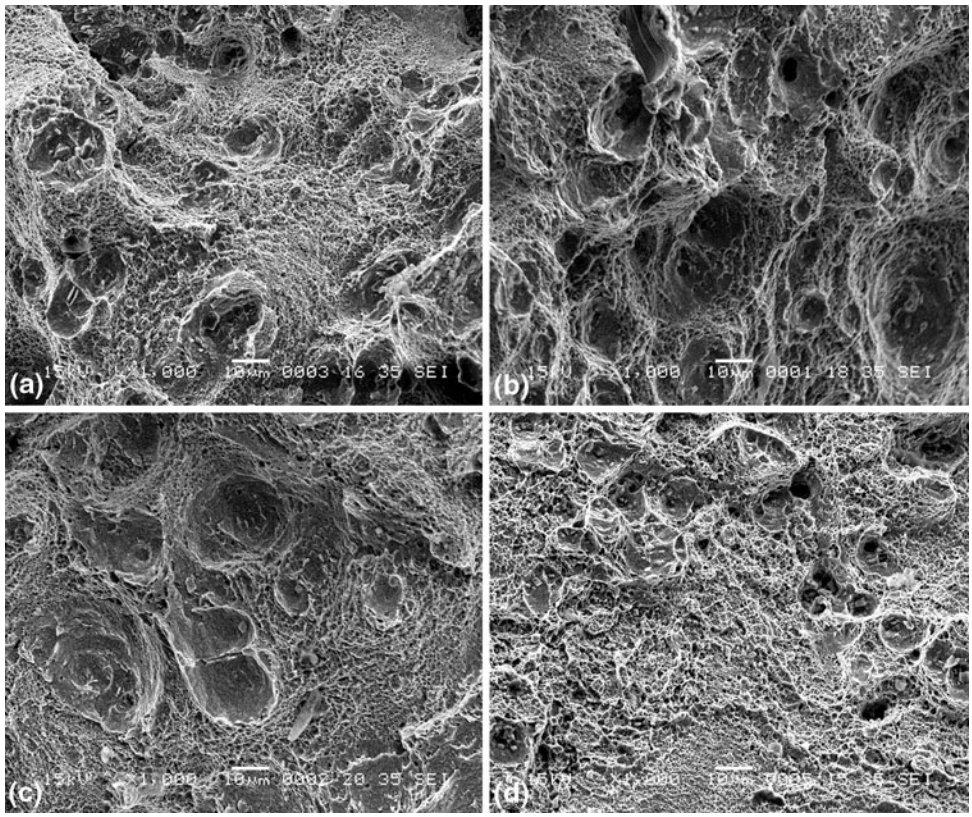

Fig. 3 SEM fractographs of Charpy V-notch specimens showing (a) ductile fracture with coarser dimples and voids in S1 after 2nd cycle, (b) ductile fracture with large dimples in S5 after 2nd cycle, (c) ductile fracture with dimples in S6 after 2nd cycle, and (d) brittle cleavage fracture with small dimples in S7 after 2nd cycle

cooling to room temperature transformed into stable γ. At prolonged aging times at temperatures of about 773 K, reversion to γ was noticed to increase along with the formation of Fe_2Mo precipitate. The γ formed due to thermal cycling was found thermally and mechanically stable, since cooling down to liquid nitrogen temperature and mechanical grinding did not affect its existence. Figure 4(e) and (f) shows the micrographs taken at higher magnification which reveals very fine lath structure with high dislocation density on which precipitates (probably Ni_3Mo or Fe_2Mo) have been formed. Moreover, subgrain structure of lath martensite (i.e. packets within grains) were also visible in high-magnification micrographs. However, precipitates were not visible in optical micrographs due to their finer sizes. Austenite seems to be interspersed within the martensite blocks and aligned along the direction of laths (Fig. 4e).

Figure 5 shows the scanning electron micrographs of the cyclic aged samples, revealing the well-defined morphology of fine lath martensite and distribution and dispersion of γ (light regions) within the laths nucleated in a definite direction along the laths. Well-defined sub-cell arrangement of martensite laths was revealed in Fig. 5(b). Austenite phase is surrounded by dark etched region due to the existence of segregated elements in these regions which etches dark. The cyclic aging treatment at 773 K for longer time periods was found to produce a greater degree of γ reversion. Structure also shows dispersion of very fine precipitates. It was further observed that with increasing aging cycles, microstructure became denser because of precipitation of different intermetallics (coherent, semi-coherent, and non-coherent equilibrium precipitates), coarsening of particles precipitated earlier during 1st aging cycle, and segregation of alloying elements and reversion of γ all occurring at the same time. Reversion of inter-lath γ was also confirmed by EDX analysis and x-ray diffraction technique. Average composition of γ phase after EDX was found to be about 19.5% Ni, 8.3% Co, 9.5% Mo, and 0.95% Ti. High Ni content lowers the austenite start (A_s) temperature and increases the stability of γ at room temperature. It is known that thermal cycling in α + γ region stabilizes the reverted γ (Ref 28), but in this study, it is observed that thermal cycling below A_s temperature also stabilizes the γ phase. Mo was found to segregate to a greater extent as a result of thermal cycling. This local enrichment of Mo indicates that the Ni_3Mo precipitates were dissolved and replaced by Fe_2Mo precipitate. This results in Ni-rich regions which transformed to γ on subsequent cooling.

X-ray diffraction was carried out on suitably prepared sheet samples after each aging cycle to measure the relative amount of austenite and martensite phases; however, results of only selected samples with austenite (111)γ, (200)γ and martensite $(110)_M$, $(200)_M$ peaks are shown in Fig. 6.

The diffraction peaks corresponding to the planes of each phase were compared to one another. The analyzed peaks were $(110)_M$, (111)γ, $(200)_M$, and (200)γ. The average values of all the compared diffraction peaks were calculated by direct comparison method to minimize the effect of preferential direction. It was observed from the results of XRD that in some cases the (200)γ peak was absent in the diffraction pattern. The maximum amount of γ was found to be 22.88% in S6 sample

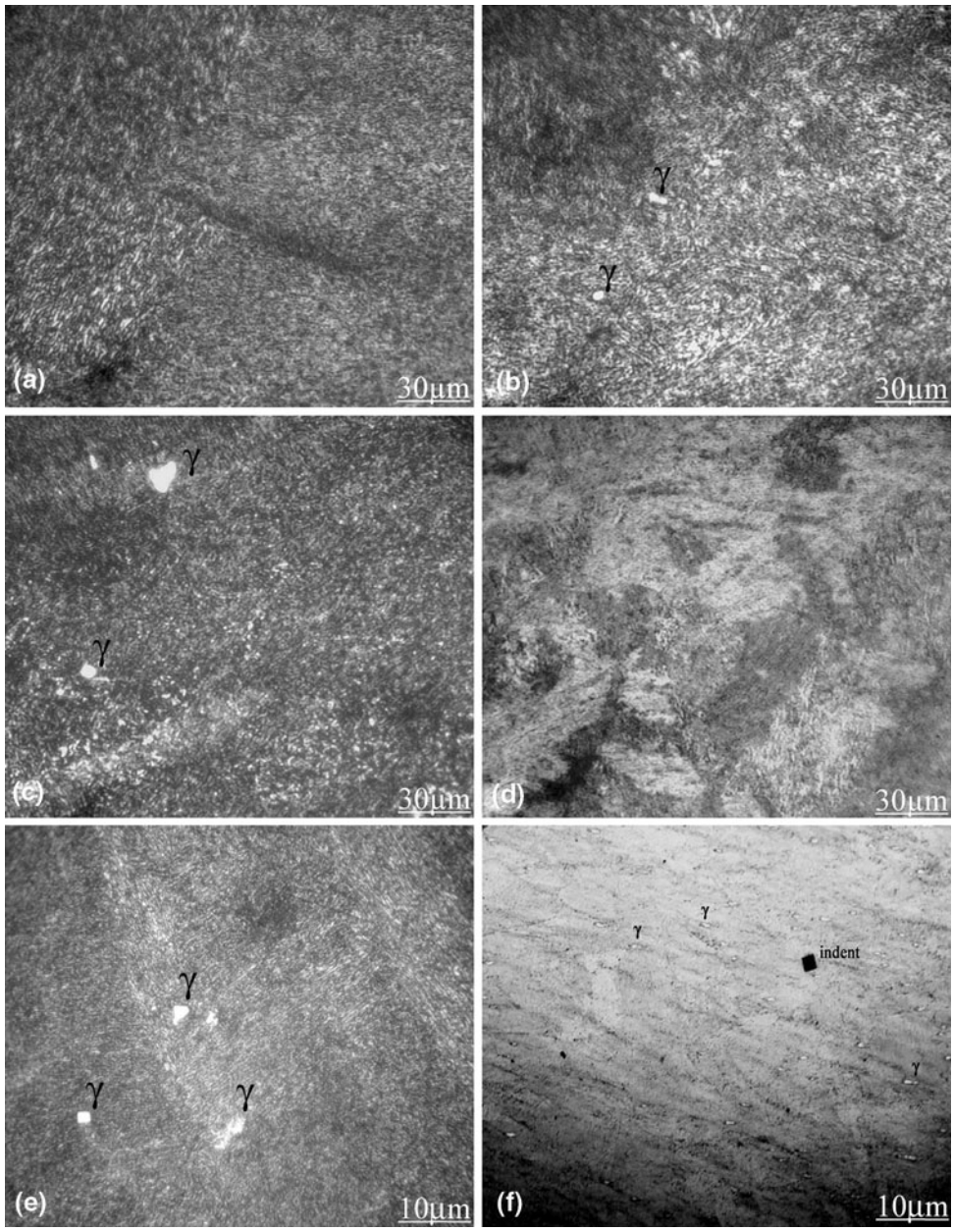

Fig. 4 Optical micrographs of maraging steel 250 samples after different cyclic aging treatments and aging times (a) S1 after 1st cycle, (b) S1 after 2nd cycle, (c) S3 after 2nd cycle, (d) S7 after 2nd cycle, (e) S1 after 2nd cycle (at higher magnification), and (f) S5 after 2nd cycle (at higher magnification)

after 4th aging cycle (as shown in Fig. 6d). In most cases after cyclic aging treatments, the amount of γ was found to be in the range of 10-15%. General trend was an increase in % γ with increasing aging cycles (e.g. 10.4% in S2 after 2nd aging cycle, 13.85% in S2 after 4th aging cycle was calculated). However, it was observed that the samples aged for longer period in 1st cycle yield lower amount of γ after each successive cycle. Similar behavior, regarding % γ, was also noted in the results of microscopy. The lattice parameters (*a*) of martensite and austenite (γ) were also calculated and found to be 2.88 and 3.59 Å, respectively. Furthermore, the increase in lattice parameters of both martensite and γ phases was also observed in some cases and was attributed to the local enrichment of alloying elements in respective phase. For instance, lattice parameter of γ was calculated up to 3.70 Å and martensite up to 2.90 Å. Similar trend regarding lattice parameters of both phases was also reported earlier (Ref 29).

4. Discussion

In virtually all precipitation hardening alloys, final set of mechanical properties are achieved by subjecting the solution annealed alloy to an aging treatment at elevated temperature below the solvus temperature particularly for that alloy system (or at room temperature in case of natural aging, e.g. some aluminum alloys) followed by cooling in suitable media

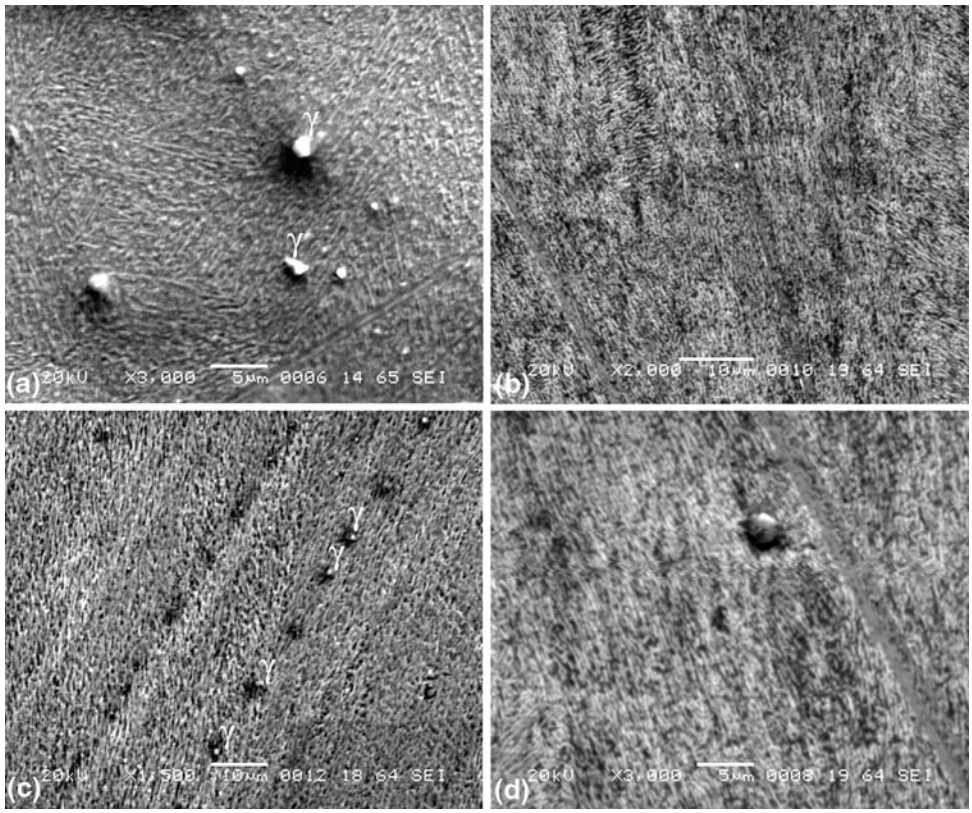

Fig. 5 SEM micrographs of cyclic aged samples showing lath martensite with white small pools of inter-lath reverted austenite (γ) and dispersion of fine intermetallic precipitates in (a) S7 after 2nd cycle, (b) S1 after 3rd cycle, (c) S5 after 3rd cycle, and (d) S1 after 4th cycle

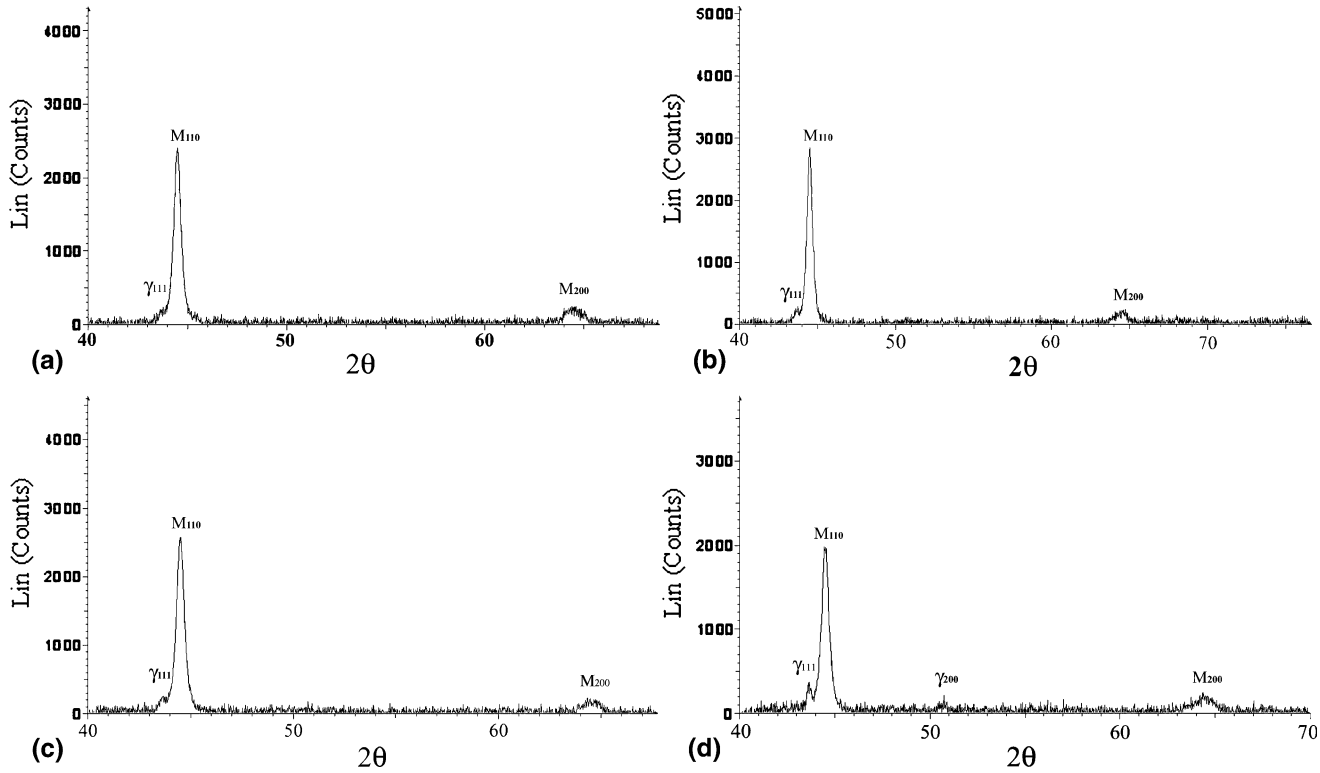

Fig. 6 X-ray diffractograms of cyclic aged samples after different number of aging cycles for different time periods (a) S2 after 2nd aging cycle, (b) S4 after 2nd aging cycle, (c) S2 after 4th aging cycle, and (d) S6 after 4th aging cycle

(mostly air). Similarly, in case of 18% Ni maraging steel grade 250, the peak hardness and strength are achieved by subjecting the solution annealed part to an aging temperature of 753 K for reasonably period of time (usually 3-8 h) followed by cooling in air at room temperature. In maraging steel 250 sheet used in this investigation, hardness in solution annealed condition was approximately 300 HV and ASTM grain size number was approximately 8 (grain diameter about 20-23 μm). However, after standard aging treatment, the nominal hardness (i.e. >525 HV) and strength (i.e. >1750 MPa) were not achieved. Even aging for longer periods and at higher temperature did not significantly improve the properties. Rather, aging at higher temperature or at longer time periods resulted in softening. The main cause of softening was found to be reversion of austenite, as known earlier (Ref 5, 6). Decrease in hardness when the alloy was overaged was also due to coarsening of intermetallic precipitates, but the effect of austenite reversion on hardness was more pronounced as compared to coarsening of precipitates in 18% Ni maraging steels. The hardening behavior of maraging steels depends on several factors like type, degree, distribution and shape of hardening precipitates. It is known that orthorhombic Ni_3Mo metastable precipitates are responsible for the initial hardening, whereas the peak strength is obtained by the presence of fine distribution of equilibrium hexagonal closed-pack (hcp) Fe_2Mo precipitates in maraging steel 250 (Ref 1, 8). Precipitation reactions in highly alloyed maraging steels are rather complex and a significant amount of research has been devoted to the study of this phenomenon. The reason for lower hardness and strength level achievable in this maraging steel 250 sheet was expected to be due to incomplete precipitation reactions and comparatively coarser grain size, i.e. approximately 8 (grain diameter 24 μm). ASTM grain size number was found to be 9 (grain diameter about 16-18 μm) in other sheet having different heat numbers but similar composition and production route in which the required mechanical properties were achieved after single step aging treatment at 753 K for 3 h. Moreover, microstructural examination revealed quite non-homogeneous structures (typical lath-martensitic structure was also not observed) in this sheet after aging. The exact reason for this behavior was not included in the scope of this work and therefore not investigated. However, the possible reason in our opinion for this behavior was improper heat treatment procedures (e.g. insufficient or incomplete homogenization treatment prior to solution annealing treatment) carried out during production. This type of heat is often called "Dead Heat". A dead heat is one that does not respond to thermal treatment for achieving an appropriate structure, property, or composition (Ref 30). It was interesting to undertake a detailed experimental work to obtain the required mechanical properties and structures in this steel. In many research works on maraging steels, it was shown that an improvement in mechanical properties can be achieved by thermal cycling either in single γ phase or dual $\alpha + \gamma$ phase region (mainly to refine the grain size) followed by aging at 753 K for 3 h (Ref 14-23). However, it was costly, difficult, and time-consuming to subject this steel to thermal cyclic treatments at higher temperatures; therefore, in this study, four thermal aging cycles were planned at 753 and 773 K for varying time periods with air cooling in between each cycle as shown in Table 2 and their effects on mechanical properties and microstructures were analyzed.

Hardness and strength were found to increase suddenly (i.e. due to absence of incubation period in maraging steel which is the result of supersaturation of solute elements and heterogeneous nucleation on dislocations) with increase in aging time for all cycles; however, a decline in curves was observed for intermediate aging times (i.e. 1-1.25 h) as seen in Fig. 1(a) and (b). Furthermore, gain in hardness and strength was obtained with increasing aging cycles. Peak hardness and strength of 540 HV and 1775 MPa was achieved after 4th aging cycle at 773 K in sample S3. It was further observed that hardness and strength did not increase above a certain limit when subjected to cyclic aging at 753 K, no matter how many cycles were given. Further rise in properties was observed only when the temperature of aging cycles was increased to 773 K. The possible reason for this behavior in our opinion is that initial increase in hardness at 753 K was caused by the precipitation of Ni_3Mo precipitates, while further gain in hardness was achieved at 773 K by precipitation of Fe_2Mo precipitate (Ref 1, 8, 10). Another contribution to the hardness possibly comes from ordering of the martensite matrix. Loss in hardness and strength were observed in some samples after 4th aging cycle at 773 K and associated mainly with the reversion of γ as detected by optical and scanning electron microscopy and XRD. Ductility (as measured in terms of %elongation) and impact absorbed energy were found to decrease with increase in hardness and strength (Fig. 1c, d). For most samples, approximately 10-15% reductions in ductility and 35-45% reductions in impact absorbed energy were observed. Average elongation about 7.2% and impact absorbed energy about 22 J were attained in S4 after 4th aging cycle. Elongation and impact absorbed energy at peak hardness were found to be 6.3% and 10 J, respectively. From impact testing results, it was observed that thermal aging cycles drastically affect the impact toughness of maraging steel 250. It can be assumed that a significant drop in impact absorbed energy with increasing number of aging cycles is due to the precipitation of a large number of brittle hardening particles which provide potential sites for crack nucleation. However, by varying the cyclic aging conditions, it is possible to improve the impact toughness characteristics.

Fractographic observations made on fractured Charpy V-notch specimens of high impact energies by stereomicroscope and SEM show ductile transgranular fracture with voids and large dimples in samples (Fig. 2a, b and 3a, b). Cracks were thought to nucleate either at inclusions or probably at precipitates which then grow with increasing stress into void. Voids could also be nucleated at reverted γ. Formation of microvoids was expected to lead to coalescence into large (coarse) dimples followed by complete separation into two, as seen in Fig. 3(a) and (b). On the other hand, samples with lower impact absorbed energies were fractured in brittle transgranular manner with microvoids and few dimples of smaller size on surface (Fig. 2e, f and 3d). The small dimples probably nucleated at overaged particles. It is clear from fractography that the mode of fracture changes from ductile to brittle cleavage with the increase in strength with increasing aging cycles.

Examination of microstructures of steel after cyclic aging shows bcc lath martensitic matrix with high dislocation density on which fine precipitates are nucleated (Fig. 4). With increase in aging cycles, the structures become dense due to precipitation of intermetallic compounds. No marked difference was observed in morphology of martensite laths with increasing aging cycles. However, it was interesting to see the reversion of γ on lath boundaries as a result of aging cycles in optical micrographs shown in Fig. 4(b), (c), (e), and (f). Morphology,

size, shape, and distribution pattern of γ were observed at higher magnification in SEM micrographs (Fig. 5). Austenite was found to nucleate as small patchy regions at martensite lath boundaries along the direction of lath (Fig. 5a, c) and there must exist a definite crystallographic orientation relationship with adjacent laths. However, presence of γ at prior austenite grain boundaries was not detected. Austenite phase is normally observed in overaged steels formed by diffusion mechanism as a consequence of isothermal treatment above A_s temperature (Ref 7, 9, 25, 31, 32). Formation of reverted γ is also known to occur by shear mechanism as a result of thermal cycling in the dual α + γ phase region (Ref 20-23) or as a result of thermal cycling between α → γ (Ref 14-19). The formation of reverted γ as a result of cyclic aging (below A_s temperature) was not known earlier. However, in this investigation, average 10-15% γ was detected by x-ray diffraction (Fig. 6) and the amount of γ was found to increase with increasing aging cycles up to 23% maximum (Fig. 6d). Moreover, formation of reverted γ was found to accelerate at higher aging temperature (i.e. 773 K) and for longer time period. Reversion of γ could occur as a result of thermal cycling which causes segregation of γ stabilizing elements, i.e. Ni and Mo (Ref 33). Moreover, precipitation of Fe_2Mo phase at higher temperature is accompanied by depletion of Fe from the martensite matrix, thus raising the relative Ni content in some regions (Ni-rich zones were formed), which transformed into γ upon cooling to room temperature due to higher A_s temperature. Thermal cycling also enhanced segregation of Mo in maraging steel, as confirmed by EDX analysis and results in the formation of Mo-rich laths (having very low M_s and A_s temperatures). Partitioning of solute elements forming an alloy-enrich (i.e. localized increase in concentration of certain elements) and alloy-depleted zone due to thermal cycling was also indicated by the change in lattice parameter (a). Average values of lattice parameter of martensite and γ were found to be about 2.88 and 3.59 Å, respectively, but with increase in solute concentrations due to thermal aging cycles the lattice parameter of martensite and γ went up to 2.90 and 3.70 Å, respectively. Zones rich in Ni and Mo retain the γ at room temperature and below it (Ref 33). The rate of formation and the vol. fraction of reverted γ increase with an increase in Ni and Mo contents and decrease with an increase in Co and Ti contents (Ref 8). Reverted γ rich in Ni and Mo content formed due to thermal cycling was found thermally and mechanically stable. The regular mechanically unstable γ is known to be rich in Ni only, whereas the segregated reverted γ mechanically stable one is rich in both Ni and Mo. This finding is in agreement with the observation of other researchers (Ref 31, 33). Microstructural examination and XRD results therefore strengthen the assumption that improvement in mechanical properties with aging cycles specifically at 773 K is attributed to the formation of lave Fe_2Mo equilibrium phase (precipitation of more than one hardening phase cannot be neglected). The presence of reverted γ in the structure also indicates that the precipitation of Fe_2Mo phase has occurred, since both precipitation of Fe_2Mo and reversion of γ occur simultaneously. However, the effect of thermal aging cycles on hardening reactions needs further detailed investigation.

Thus, it was observed that mechanical properties could be improved by subjecting the maraging steel 250 to cyclic aging treatments. However, the time and temperature of aging cycles are important and need to be tailored for achieving required combinations of properties, particularly toughness-related properties. Analyzing the results presented, we managed to choose a cyclic aging treatment that ensures the required level of mechanical properties and microstructure in the studied steel, i.e. approximately 550 HV hardness, 1800 MPa tensile strength with >6% elongation and <12% γ in bcc lath martensite. However, the impact absorbed energy at this strength level was 10 J and further detailed investigation is required to improve impact properties. The maraging steel 250 achieved these properties only after aging for 0.5-0.75 h during 1st aging cycle at 753 K. Even a deviation of few minutes in aging time of 1st cycle causes considerable changes in the final mechanical properties of the steel after 4th aging cycle. The effect of aging time of 1st cycle on final properties is still not known and needs further research.

5. Conclusions

1. The application of cyclic aging treatments can significantly improve the mechanical properties of maraging steel 250. Maraging steel of desired optimum mechanical properties and structure can be produced by varying the temperature, time, and cycles of aging.
2. Increase in hardness up to 20% and strength up to 25% with corresponding decrease in ductility and impact resistance were observed with increasing aging cycles up to 4. Peak hardness of 540 HV and strength about 1775 MPa were achieved in S3 after 4th aging cycle at 773 K. However, elongation and impact resistance, at peak hardness, were found to be 6.3% and 10 J, respectively.
3. With the increase in hardness and strength due to increasing aging cycles, the mode of fracture changes from ductile dimple-like fracture to brittle cleavage fracture. SEM fractographs showed transgranular fracture with microvoids and dimples in all cases. However, coarser dimples in fracture were observed at higher impact energies as compared to small dimples with microvoids at lower impact energies.
4. Optical and scanning electron micrographs showed fine bcc lath martensite with dispersion of very fine intermetallic precipitates. Precipitates are expected to be Ni_3Mo at lower temperatures and Fe_2Mo at higher temperatures and longer times. No change in lath martensitic morphology was observed with increasing aging cycle. However, matrix structure becomes more dense and heterogeneous due to complex precipitation reactions occurring with increase in aging cycles.
5. Inter-lath reverted γ was observed in the microstructure after cyclic aging. The presence of γ was confirmed by EDX analysis and x-ray diffraction technique. The formation of reverted γ is associated with the formation of Ni- and Mo-rich regions having lower M_s and A_s temperatures and therefore transform in a γ rather than martensite. Amount of γ was found to increase with increasing aging cycles. Higher aging temperatures for longer time periods also promote γ formation. Maximum amount of γ was calculated to be 22.88% after 4th aging cycle at 773 K.

Acknowledgments

The authors thank Mr. Muhammad Saraf (Deputy Chief Manager) and Dr. Sajid Mirza (Senior Chief Manager) for their valuable suggestions and Mr. Raza Hussain (Chairman SUPARCO)

for their guidance and provision of facilities. The authors also like to thank Mr. Badar-ul-Hassan (Technical Officer) for his technical assistance and discussion throughout the experimental work.

References

1. G.P. Miller and W.L. Mitchell, Structure and Hardening Mechanisms of 18% Nickel-Cobalt-Molybdenum Maraging Steels, *J. Iron Steel Int.*, 1965, **203**, p 899–904
2. A. ul Haq, F.H. I-Imhnfi, and A.Q. Khan, Physical and Mechanical Properties of Maraging Steels, *Pak. Steel J.*, 1986, **28**, p 87–90
3. K.V. Rajkumar, Anish Kumar, T. Jayakumar, Baldev Raj, and K.K. Ray, Characterization of Aging Behavior in M250 Grade Maraging Steel Using Ultrasonic Measurements, *Metall. Mater. Trans. A*, 2007, **38A**, p 236–243
4. Nickel Development Institute, 18 Percent Nickel Maraging Steels: Engineering Properties, Publication No. 4419, 1976, p 6–7
5. A.F. Edneral and M.D. Perkas, Structural Changes During Aging of Fe-Ni-Mo Alloys, *Fiz. Met. Metalloved.*, 1970, **28**(5), p 862
6. A.F. Edneral and M.D. Perkas, The Aging of Martensite of N18K9M5T Steel, Translated from *Metallovedenie i Termicheskaya Obrabotka Metallov*, 1968, **6**, p 18–19
7. F. Habiby, T.N. Siddiqui, S.H. Khan, A. ul Haq, and A.Q. Khan, Austenite Determination by Eddy Current Measurements in a Maraging Steel, *NDT&E Int*., 1992, **25**(3), p 145–146
8. V.K. Vasudevan, S.J. Kim, and C. Marvin Wayman, Precipitation Reactions and Strengthening Behavior in 18 Wt Pct Nickel Maraging Steels, *Metall. Trans. A*, 1990, **21A**, p 2655–2668
9. M. Ahmed, K. Hasnain, I. Nasim, and H. Ayub, Magnetic Properties of Maraging Steels in Relation to Nickel Concentration, *Metall. Mater. Trans. A*, 1995, **26A**, p 1869–1876
10. V.E. Laz'ko, Regular Changes in the Strength of Maraging Steels Upon Complex Alloying with Cobalt, Nickel and Molybdenum, Translated from *Metallovedenie i Termicheskaya Obrabotka Metallov*, 2001, **2**, p 25–28
11. L.N. Belyakov, V.L. Nikol'skaya, and S.S. Ryzhak, The $\alpha \rightarrow \gamma$ Transformation in Maraging Steel N18K9M5T, Translated from *Metallovedenie i Termicheskaya Obrabotka Metallov*, 1968, **6**, p 26–32
12. N.F. Lashko, L.V. Zaslavskaya, V.L. Nikol'skaya, and G.G. Solov'eva, Phase Composition, Structure and Properties of Maraging Steel Kh14K9N6M5, Translated from *Metallovedenie i Termicheskaya Obrabotka Metallov*, 1974, **10**, p 39–42
13. M.E. Blanter and L.A. Kovaleva, Mechanical Properties and Nature of Strengthening of Maraging Steels, Translated from *Metallovedenie i Termicheskaya Obrabotka Metallov*, 1969, **10**, p 30–33
14. G.A. Beresnev, L.D. Pilikina, and Yu.I. Kataev, Mechanical Properties of Plates of Maraging Steel NI8K9M5T, Translated from *Metallovedenie i Termicheskaya Obrabotka Metallov*, 1970, **2**, p 60–61
15. O.V. Abramov, A.I. Il'in, and V.M. Kardonskii, Effect of Heat Treatment on Mechanical Properties of Maraging Steel, Translated from *Metallovedenie i Termicheskaya Obrabotka Metallov*, 1983, **4**, p 43–46
16. Yu.V. Shakhnazarov, V.V. Tikhomirov, N.I. Vorob'eva, and V.D. Popov, The Heat Treatment of Large Forgings of N18K9M5T Maraging Steel, Translated from *Metallovedenie i Termicheskaya Obrabotka Metallov*, 1972, **2**, p 53–55
17. T.M. Maslakova, Effect of Thermal Cycling on ($\gamma \rightarrow \alpha$) Properties of Maraging Steel, Translated from *Metallovedeuie i Termicheskaya Obrabotka Metallov*, 1978, **12**, p 23–27
18. S.S. Ryzhak, O.K. Revyakina, V.V. Sachov, and Ya.M. Potak, Heat Treatment of Maraging Steel 00N18K9M5T, Translated from *Metallovedenie i Termieheskaya Obrabotka Metallov*, 1968, **6**, p 20–22
19. V.M. Kardonskii, Stabilization of Austenite During the Reverse $\alpha \rightarrow \gamma$ Transformation, *Fiz. Met. Metalloved.*, 1975, **5**(40), p 1010
20. M.Kh. Shorshorov, V.I. Aatipov, E.D. Kudinov, and E.I. Mikhaleva, Effect of Thermal Cycling in Welding on the Structure and Phase Composition of the Heat-Affected Zone in Maraging Steel, Translated from *Metallovedenie i Termieheskaya Obrabotka Metallov*, 1973, **11**, p 62–63
21. E.D. Kudinov, E.I. Mikhaleva, A.A. Pigenko, and P.A. Prokhorov, Properties of the Heat-Affected Zone of Maraging Steels in Relation to Thermal Cycles During Welding, Translated from *Metallovedenie i Termieheskaya Obrabotka Metallov*, 1972, **10**, p 23–26
22. M.M. Shtrikman, I.P. Kapranova, and E.T. Romanova, Structure and Properties of Welds in Maraging Steel N18K9M5T, Translated from *Metallovedenie i Termicheskaya Obrabotka Metallov*, 1972, **10**, p 18–22
23. I.V. Pestov, A.Ya. Maloletnev, M.D. Perkas, and A.F. Edneral, Low-Cycle Impact Fatigue Strength of Steel NI8K9M5T with a Biphase $\alpha + \gamma$ Structure, Translated from *Metallovedenie i Termicheskaya Obrabotka Metallov,* 1981, **4**, p 28–31
24. B.D. Cullity and S.R. Stock, *Elements of X-Ray Diffraction*, 3rd ed., Prentice Hall, New Jersey, 2001
25. C.A. Pampillo and H.W. Paxton, The Effect of Reverted Austenite on the Mechanical Properties and Toughness of 12 Ni and 18 Ni (200) Maraging Steels, *Metall. Trans.*, 1972, **3**, p 2895–2903
26. C.R. Shamantha, R. Narayanan, K.J.L. Iyer, V.M. Radhakrishnan, S.K. Seshadri, S. Sundararajan, and S. Sundaresan, Tensile Properties and Fracture Toughness of 18Ni (250 Grade) Maraging Steel Weldments, *Sci. Technol. Weld. Join.*, 2000, **5**(5), p 329–337
27. O.V. Abramov, A.I. Il'in, and V.M. Kardonskii, Effect of Heat Treatment on the Mechanical Properties of Maraging Steel, Translated from *Metallovedenie i Termicheskaya Obrabotka Metallov*, 1983, **4**, p 43–46
28. A.M. Hall and C.J. Slunder, *The Metallurgy, Behaviour and Applications of 18 Ni Maraging Steel*, NASA, SP-5051 Washington DC, 1968
29. J.M. Pardal, S.S.M. Tavares, M.P. Cindra Fonseca, H.F.G. Abreu, and J.J.M. Silva, Study of the Austenite Quantification by X-Ray Diffraction in the 18Ni-Co-Mo-Ti Maraging 300 Steel, *J. Mater. Sci.*, 2006, **41**, p 2301–2307
30. C. Hays and R.P. Stemmler, Banding of MAR-Aging Steel, *J. Mater. Eng. Perform.*, 2000, **9**(2), p 147–152
31. Y. Katz, H. Mathias, and S. Nadiv, The Mechanical Stability of Austenite in Maraging Steels, *Metall. Trans. A*, 1983, **14A**, p 801–808
32. S. Floreen and R.F. Decker, Ed., *Source Book on Maraging Steel*, ASM International, Metals Park, OH, 1979
33. M. Ahmed, I. Nasim, and S.W. Husain, Influence of Nickel and Molybdenum on the Phase Stability and Mechanical Properties of Maraging Steels, *J. Mater. Eng. Perform.*, 1994, **3**(2), p 248–254